LETTER

doi:10.1038/nature14092

Anomalous dispersions of 'hedgehog' particles

Joong Hwan Bahng[1], Bongjun Yeom[2], Yichun Wang[1], Siu On Tung[3], J. Damon Hoff[4] & Nicholas Kotov[1,2,3,5,6]

Hydrophobic particles in water and hydrophilic particles in oil aggregate, but can form colloidal dispersions if their surfaces are chemically camouflaged with surfactants, organic tethers, adsorbed polymers or other particles that impart affinity for the solvent and increase interparticle repulsion[1,2]. A different strategy for modulating the interaction between a solid and a liquid uses surface corrugation, which gives rise to unique wetting behaviour[3–5]. Here we show that this topographical effect can also be used to disperse particles in a wide range of solvents without recourse to chemicals to camouflage the particles' surfaces: we produce micrometre-sized particles that are coated with stiff, nanoscale spikes and exhibit long-term colloidal stability in both hydrophilic and hydrophobic media. We find that these 'hedgehog' particles do not interpenetrate each other with their spikes, which markedly decreases the contact area between the particles and, therefore, the attractive forces between them. The trapping of air in aqueous dispersions, solvent autoionization at highly developed interfaces, and long-range electrostatic repulsion in organic media also contribute to the colloidal stability of our particles. The unusual dispersion behaviour of our hedgehog particles, overturning the notion that like dissolves like, might help to mitigate adverse environmental effects of the use of surfactants and volatile organic solvents, and deepens our understanding of interparticle interactions and nanoscale colloidal chemistry.

We imparted strong corrugation onto the surface of carboxylated polystyrene microspheres (μPSs) by attaching rigid zinc oxide (ZnO) nanoscale spikes ('nanospikes'). This involves initial absorption of positively charged ZnO nanoparticles (NPs) onto the negatively charged μPSs and subsequent growth of ZnO nanowires using established protocols[6]. The resultant hedgehog particles combine micro- and nanoscale structural features (Fig. 1a), and their geometrical and topographical specifications can be adjusted by changing the growth conditions to modify the surface densities, lengths and diameters of nanospikes and the μPS diameters (Fig. 1b–e, Supplementary Information section 1 and Supplementary Figs 2–5).

As-made hedgehog particles, with their polar ZnO surfaces, are highly hydrophilic. They form excellent dispersions in water (Fig. 1f, l) and other hydrophilic solvents. When rendering the hedgehog particles hydrophobic by silanization of the ZnO nanospikes with (7-octen-1-yl)

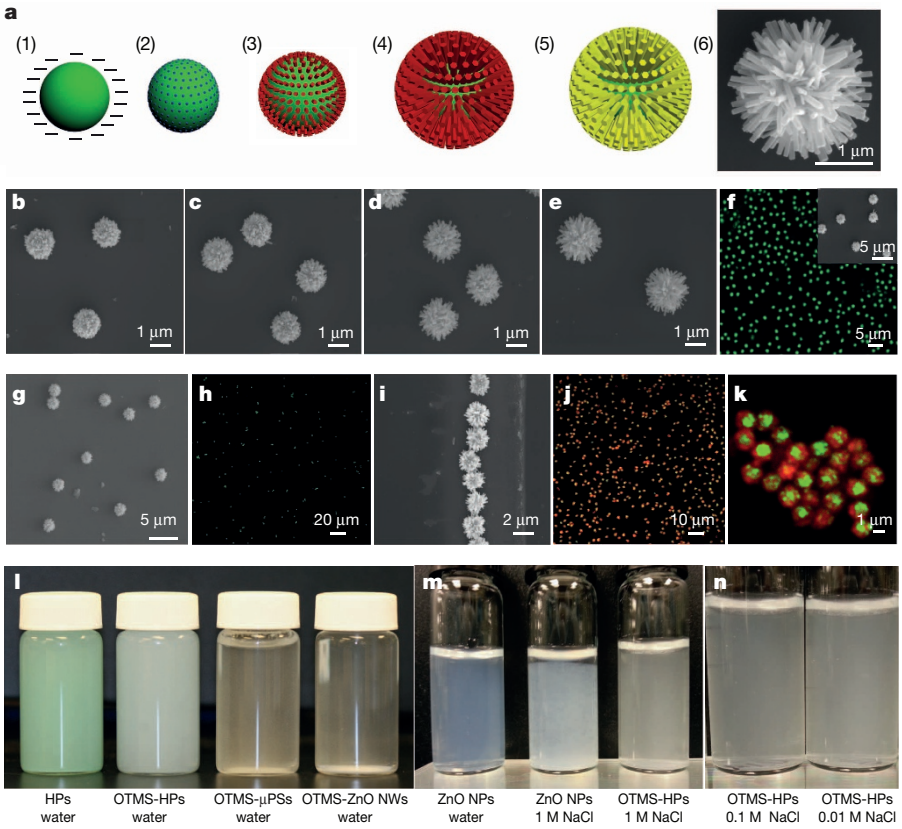

Figure 1 | Hedgehog particles. **a**, Negatively charged, carboxylate-terminated μPSs are used as core templates (1) on which positively charged ZnO NPs are adsorbed (2). ZnO nanospikes are grown from ZnO nanoparticles (3) to a designed length (4, 6). Hedgehog particles are rendered hydrophobic by exposure to OTMS or PFTS (5). **b–e**, SEM images of hedgehog particles with different ZnO nanospike lengths: 0.19 μm (**b**), 0.27 μm (**c**), 0.4 μm (**d**), 0.6 μm (**e**). **f**, Confocal microscopy of an aqueous dispersion of hydrophilic hedgehog particles with fluorescently labelled μPSs. Inset, SEM image for the same hedgehog particles. **g**, **h**, SEM (**g**) and confocal microscopy (**h**) of an aqueous dispersion of OTMS-HPs. **i**, SEM image of particles from the bulk of an aqueous OTMS-HP dispersion collected five days after initial preparation. **j**, **k**, Confocal microscopy images of fluorescent OTMS-HPs (green, $\lambda_{max} = 486$ nm) with adsorbed hydrophobic CdSe nanoparticles (red, $\lambda_{max} = 655$ nm) in an aqueous dispersion (**j**) and in the dried state (**k**). **l**, Photographs of aqueous dispersions of (left to right) hydrophilic hedgehog particles (HPs) with green-dyed μPSs, OTMS-HPs, OTMS-μPSs and OTMS-ZnO nanowires (NWs). **m**, Photographs of (left to right) ZnO nanoparticles (NPs) in water, ZnO nanoparticles in 1 M NaCl, and OTMS-HPs in 1 M NaCl. **n**, Photographs of OTMS-HPs in (left to right) 0.1 M NaCl and 0.01 M NaCl.

[1]Department of Biomedical Engineering, University of Michigan, 1107 Carl A. Gerstacker Building, 2200 Bonisteel Boulevard, Ann Arbor, Michigan 48109, USA. [2]Department of Chemical Engineering, University of Michigan, 3074 H.H. Dow Building, 2300 Hayward Street, Ann Arbor, Michigan 48109, USA. [3]Macromolecular Science and Engineering Program, University of Michigan, 3062C H.H. Dow Building, 2300 Hayward Street, Ann Arbor, Michigan 48109, USA. [4]Single Molecule Analysis in Real Time (SMART) Center, Ann Arbor, Michigan 48109, USA. [5]Department of Material Science and Engineering, University of Michigan, 3074 H.H. Dow Building, 2300 Hayward Street, Ann Arbor, Michigan 48109, USA. [6]Biointerfaces Institute, University of Michigan, North Campus Research Complex, 2800 Plymouth Road, Ann Arbor, Michigan 48109, USA.

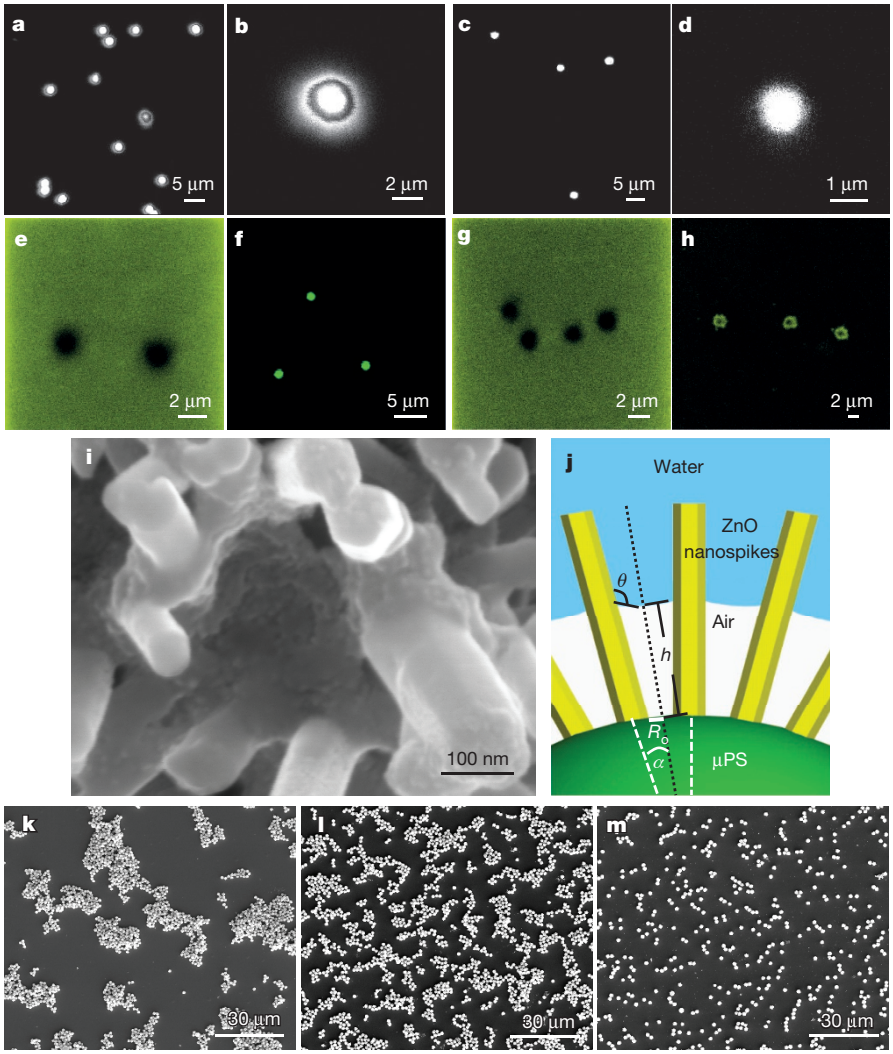

Figure 2 | Interface between hydrophobic hedgehog particles and water. **a**–**h**, Confocal microscopy images of hydrophobic hedgehog particles labelled with hydrophobic CdSe NPs in aqueous dispersions (**a**, **b**) and hydrophilic hedgehog particles labelled with hydrophilic CdTe NPs in aqueous dispersions (**c**, **d**); hydrophobic hedgehog particles in an aqueous solution containing hydrophilic TGA-stabilized CdTe nanoparticles with green (λ_{max} = 540 nm) emission (**e**); hydrophilic hedgehog particles in an aqueous solution containing hydrophilic TGA-stabilized CdTe nanoparticles (**f**); the same sample from image **e** after five days of storage in dark (**g**); and the same sample from image **f** after five days of storage in dark (**h**). **i**, SEM image of a hydrophobic hedgehog particle with a self-assembled film of TGA-depleted CdTe nanoparticles between the ZnO nanospikes, indicating the location of the air–water interface. The hydrophobic hedgehog particles were immersed in an aqueous solution of CdTe nanoparticles for 72 h. **j**, Schematic diagram of the air–water interface, showing the experimental parameters (definitions in Supplementary Information). **k**–**m**, SEM images of aqueous dispersions of hydrophobic hedgehog particles with ZnO nanospike lengths of 0.19 μm (**k**), 0.40 μm (**l**) and 0.57 μm (**m**).

trimethoxysilane (OTMS) or 1*H*,1*H*,2*H*,2*H*-perfluorooctyltriethoxysilane (PFTS) (Supplementary Methods; spectroscopic evidence of silanization is shown in Supplementary Information section 2 and Supplementary Fig. 9c), they form stable dispersions in heptane and hexane (Supplementary Information section 2 and Supplementary Fig. 6a, b).

Surprisingly, highly corrugated OTMS-modified hydrophobic hedgehog particles (OTMS-HPs) also form dispersions in water (Fig. 1g, h, l), and hydrophilic hedgehog particles disperse in representative hydrophobic solvents such as heptane, hexane and toluene (Fig. 4a–h). This illustrates that surface topography can be used to modulate the interaction between microscale particles and disperse them in phobic solvents.

Immediately on sonicating various hydrophobic OTMS-HP and PFTS-modified hydrophobic hedgehog particle (PFTS-HP) formulations in water (Supplementary Information section 2 and Supplementary Fig. 7), we observed the formation of a precipitate on the bottom of the vial, floating aggregates on top of the liquid, and a stable opalescent dispersion. Dispersions remain stable and free of aggregation for a subset of particles for at least five days, as verified by scanning electron microscopy (SEM) (Fig. 1i) and dynamic light scattering (Supplementary Information section 2 and Supplementary Table 1). The percentage of hydrophobic hedgehog particle aggregates floating on the surface of the dispersions increased with elongation of the nanospikes (Supplementary Information section 2 and Supplementary Fig. 7a–d), but the colloidal stability of the particles dispersed in water was also enhanced (Fig. 2k–m).

To exclude the possibility that the observed behaviour arises because our samples contain a subpopulation of hydrophilic OTMS-HPs or PFTS-HPs or represent a special case of Janus colloids, that is, colloids consisting of distinct hydrophobic and hydrophilic interfacial sectors[7–9], we directly probed the hydrophobic nature of the particles after processing them into dried thin films. The filtrate of suspended OTMS-HPs exhibited high water repellency causing the droplets to roll off (the 'lotus effect'; Supplementary Information section 2, Supplementary Videos 1–3 and Supplementary Fig. 8). Further evidence is obtained by injecting hydrophobic cadmium selenide (CdSe) nanoparticles into an aqueous dispersion of OTMS-HPs: confocal and transmission electron microscopy (TEM) images show the expected anchoring of hydrophobic nanoparticles on the spikes (Fig. 1j, k, Supplementary Information section 2 and Supplementary Fig. 9d), thus confirming their hydrophobicity and the uniformity of surface derivatization. The stability of the hydrophobic hedgehog particles in aqueous dispersion did not change on CdSe adsorption.

The wetting of corrugated surfaces[4,10–12] is often attributed to a Cassie–Baxter wetting mode[13,14] and in our case could include formation of an air shell in the vicinity of the μPS core. Such trapped air bubbles[15] might provide buoyancy to the hedgehog particles, but are known to be thermodynamically unstable[16,17]. The presence of trapped air is verified by adding ethanol and observing gas evolving from the dispersion (Supplementary Video 5), and by observing, in high-resolution confocal microscopy images of the particles, concentric shells with markedly different refractive indices as would be expected if an air shell is present (Fig. 2a, b, Supplementary Information section 3 and Supplementary Fig. 10). Hydrophilic hedgehog particles in water have no air shells, and they appear under the same conditions as uniformly lit particles (Fig. 2c, d, Supplementary Information section 3 and Supplementary Fig. 11).

When adding fluorescent cadmium telluride (CdTe) nanoparticles, stabilized with hydrophilic thioglycolic acid (TGA), to an aqueous dispersion of the hydrophobic hedgehog particles, a dark zone devoid of emission around the hedgehog particles confirms the presence of a layer of air. The dimensions of the emission exclusion zones closely match the diameter of hedgehog particles (Fig. 2e). The fact that similar images were obtained after five days of storage in the dark without agitation (Fig. 2g) attests to the long-term stability of dispersions of our hydrophobic hedgehog particles in water, consistent with long-term trapping of air at macroscale corrugated surfaces[18] (Supplementary Information section 3 and Supplementary Fig. 13). Hydrophilic hedgehog particles in identical luminescent media appear as bright spots with CdTe nanoparticles localized on and between the nanospikes (Fig. 2f, h).

Strong scattering of photons and electrons by ZnO nanospikes prevents successful optical or cryogenic TEM imaging of the air–water interface within hedgehog particles, but we can locate it by taking advantage of the fact that CdTe nanoparticles can self-assemble into nanowires[19] and nanosheets[20] at interfaces[21]: a thin layer of CdTe nanoparticles that assembles more than 200 nm in from the ends of the ZnO nanospikes (Fig. 2i, Supplementary Information section 3 and Supplementary Fig. 14) pinpoints the water meniscus (Fig. 2j). This allows us to calculate an average hedgehog particle density of 0.92 g cm^{-3} (Supplementary Information section 3), which closely matches the density of water and explains the buoyancy of the particles.

We must also explain why two individual hydrophobic hedgehog particles do not coalesce on collision. To do so, we refer to the extended Derjaguin–Landau–Verwey–Overbeek (E_DLVO) theory, according to which the sum of potentials associated with van der Waals (V_{vdW}), electrical double layer (V_{DL}) and hydrophobic (V_{HB}) interactions approximate the total interaction potential (V_{E_DLVO}) between the hydrophobic hedgehog particles: $V_{E\_DLVO} = V_{vdW} + V_{DL} + V_{HB}$. Evaluating interparticle interactions in different configurations (Fig. 3a–c, Supplementary Information section 4 and Supplementary Fig. 19), we find that hedgehog-particle/hedgehog-particle pair potentials display high repulsive energy barriers of at least $14k_BT$ (k_B, Boltzmann's constant) for the outer contour of spikes ($x = 0$; Fig. 3d). Penetration of the nanospikes into the interstitial spaces of another hedgehog particle ($x < 0$) is energetically unfavourable (Fig. 3d).

Comparison of the V_{E_DLVO} for hydrophobic hedgehog particles with that for hydrophobic μPSs (Supplementary Information section 4 and Supplementary Fig. 24d) shows that the interfacial corrugations transform the overall attractive potential into a repulsive one. For hedgehog particles with short nanospikes, V_{E_DLVO} reverses such that the interaction becomes attractive (Fig. 3e), matching the experimental results in Fig. 2k. The key reason for the anomalous stability of hedgehog particle dispersions is that V_{vdW} and V_{HB} are greatly decreased for corrugated particles compared with the smooth spheres (Fig. 3f, g), owing to the drastic reduction in the contact area in the former case. The total contour area of tapered spikes represents <3% of the surface area of the smooth particles (Fig. 1a).

The colloidal stability of hydrophobic hedgehog particles in water is also enhanced by the presence of the double electric layer at the air–water interface, increasing V_{DL}. The zeta-potential (ζ) of air bubbles, which affects their electrostatic repulsion, is known to be between −35 mV (ref. 22) and −65 mV (ref. 23). Such high ζ is attributed to autoionization of water[24] that may also occur at the hydrophobic interfaces[24,25]. However, the fact that the hedgehog particle dispersion remains stable in the presence of 0.01–1.0 M NaCl, which leads to screening of electrostatic interactions and coagulation of 'normal' dispersions (Fig. 1m, n), shows that any increased electrostatic repulsion has a secondary role and that the anomalous colloidal behaviour of hedgehog particles is dominated by the reduction of attractive interactions between the particles. But limitations of Derjaguin–Landau–Verwey–Overbeek theory for high ionic strengths and nanoscale corrugated surfaces[26] may need to be considered for a more complete mechanistic explanation.

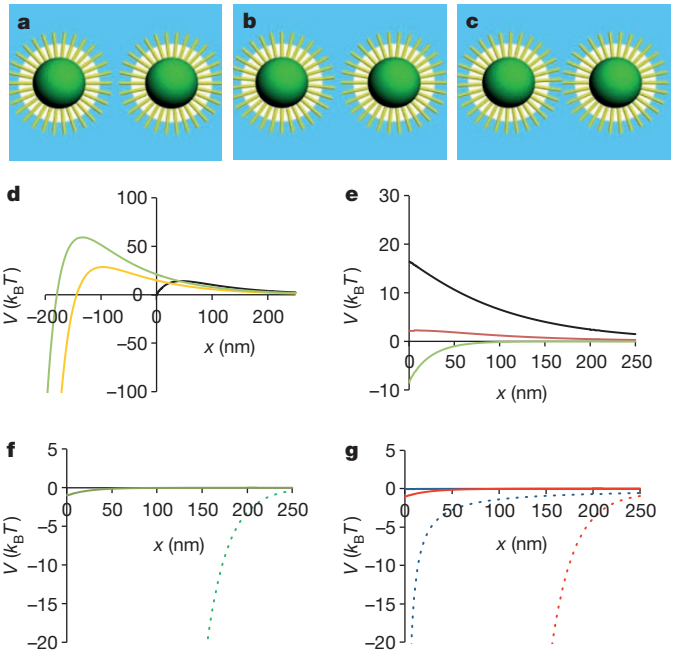

Figure 3 | Interaction potentials of hydrophobic hedgehog particles in aqueous media. **a–c**, Two general configurations, spike-to-spike (S–S; **a**) and spike-to-gap (S–G; **b**), are considered, along with the intermediate case in which the ZnO nanospikes face the side walls of opposing particles (ZS–G; **c**). **d–g**, Interaction potentials between hydrophobic hedgehog particles. **d**, Pair potentials for hydrophobic hedgehog particles in S–S ($V_{E\_DLVO,S-S}$, black), S–G ($V_{E\_DLVO,S-G}$, orange) and ZS–G ($V_{E\_DLVO,ZS-G}$, green) configurations. The negative values of x correspond to the penetration of ZnO nanospikes into the interstitial spaces of another hedgehog particle; $x = 0$ corresponds to the outer contour around the spike tips. **e**, Pair potentials ($V_{E\_DLVO,HP}$) of hydrophobic hedgehog particles in an aqueous dispersion calculated according to the E_DLVO theory for the zeta-potentials at the air–water interface with $\zeta = -65$ mV (black line) and $\zeta = -35$ mV (red line), and for hydrophobic hedgehog particles with short nanospikes from Fig. 2k (green line). **f**, Hydrophobic interaction potentials of OTMS-HPs ($V_{HB,HP}$, green) and OTMS-μPSs ($V_{HB,PS}$, dotted green). **g**, Van der Waals interaction potentials of OTMS-HPs ($V_{vdW,HP}$, blue) and OTMS-μPSs ($V_{vdW,PS}$, dotted blue) and total attractive potentials of OTMS-HPs ($V_{vdW+HB,HP}$, red) and hydrophobic OTMS-μPS ($V_{vdW+HB,PS}$, dotted red) in water.

If the drastic reduction in attractive components of the pair potential is the reason for the unusual stability of hedgehog particle dispersions, the same effect should occur in dispersions of hydrophilic colloids in hydrophobic solvents. Stable dispersions of hydrophilic hedgehog particles were obtained in heptane, hexane and toluene (Fig. 4a, Supplementary Information section 5 and Supplementary Fig. 26). SEM and confocal microscopy images (Fig. 4b–e) demonstrated non-agglomerated particles in the bulk of these dispersions and physical integrity of hedgehog particles (Fig. 4f–h). The μPS core of the hedgehog particles was dissolved in toluene, thus yielding a dispersion of hydrophilic hedgehog particle shells. As expected, ZnO nanoparticles and ZnO nanowires (Supplementary Information section 5 and Supplementary Fig. 27) do not disperse in the same solvents.

Calculations show that V_{vdW} for this type of dispersion is much reduced compared with smooth spheres, and that the overall pair potential of hydrophilic hedgehog particles in heptane is indeed repulsive with $V_{DLVO,HPs} = 1.4k_BT$ at $x = 0$ nm (Fig. 4i, j, Supplementary Information section 5 and Supplementary Fig. 28). Notably, dispersion in organic solvents lack the air layer between the spikes, and electrostatic interactions in organic solvents are not screened as in aqueous solutions and are therefore longer ranged.

The stability of our surfactant-free hedgehog particles in 'phobic' solvents offers a different perspective on scientific and technological problems related to colloidal interactions and might even enable new strategies

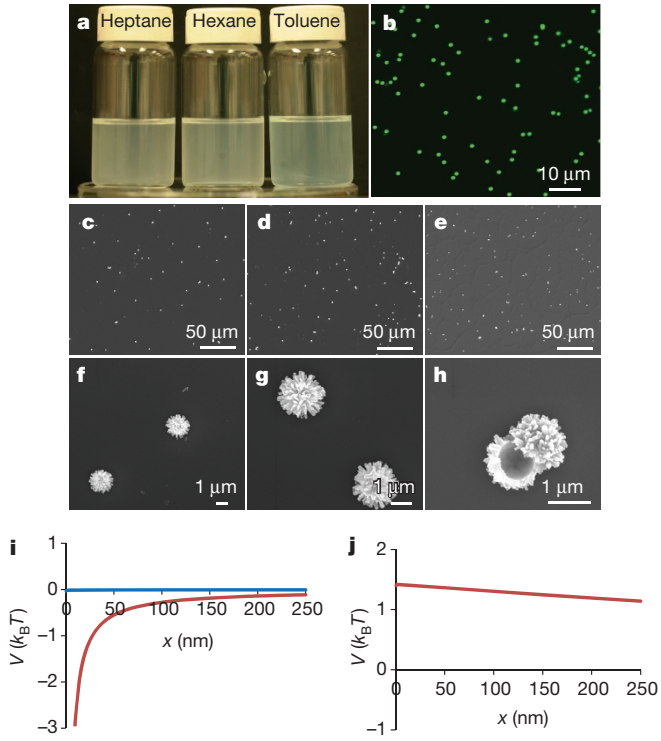

Figure 4 | Dispersion of hydrophilic hedgehog particles in hydrophobic organic solvents. **a**, Dispersions of hydrophilic hedgehog particles in (left to right) heptane, hexane and toluene. As in the case of dispersion of hydrophobic hedgehog particles in water, after sonication of hydrophilic hedgehog particles in organic solvent there was always a small amount of precipitate in the bottom of the vial. **b**, Confocal microscopy image of hydrophilic hedgehog particles in heptane. **c**–**e**, SEM images of hydrophilic hedgehog particles from dispersions in heptane (**c**), hexane (**d**) and toluene (**e**). **f**–**h**, SEM images of individual hedgehog particles in heptane (**f**), hexane (**g**) and toluene (**h**). Toluene dissolves the μPS core in the hedgehog particles, rendering dispersions of hydrophilic spiky shells. **i**, Van der Waals interaction potentials V_{vdW} of hydrophilic hedgehog particles (blue) and μPS (red) in heptane. **j**, Total pair potential V_{E_DLVO} of hydrophilic hedgehog particles in heptane.

for processing and dealing with colloids, for developing new drug delivery systems[27], and for colloidal self-assembly[9,28,29]. We also believe that the unusual solvation behaviour of hedgehog particles (contrary to the traditional expectations of particle dispersion stability in hydrophobic/hydrophilic solvents) could be used to develop efficient adsorbers, absorbers, scatterers or catalysts that need to function in both organic and aqueous media.

Received 25 October 2013; accepted 12 November 2014.

1. Israelachvili, J. N. *Intermolecular and Surface Forces* 253–413 (Academic, 2011).
2. Sperling, R. A. & Parak, W. J. Surface modification, functionalization and bioconjugation of colloidal inorganic nanoparticles. *Phil. Trans. R. Soc. A* **368,** 1333–1383 (2010).
3. Feng, L. *et al.* Super-hydrophobic surfaces: from natural to artificial. *Adv. Mater.* **14,** 1857–1860 (2002).
4. Lafuma, A. & Quéré, D. Superhydrophobic states. *Nature Mater.* **2,** 457–460 (2003).
5. Parker, A. R. & Lawrence, C. R. Water capture by a desert beetle. *Nature* **414,** 33–34 (2001).
6. Yang, P. D. *et al.* Controlled growth of ZnO nanowires and their optical properties. *Adv. Funct. Mater.* **12,** 323–331 (2002).
7. Kim, S. H., Abbaspourrad, A. & Weitz, D. A. Amphiphilic crescent-moon-shaped microparticles formed by selective adsorption of colloids. *J. Am. Chem. Soc.* **133,** 5516–5524 (2011).
8. Walther, A. & Muller, A. H. E. Janus particles: synthesis, self-assembly, physical properties, and applications. *Chem. Rev.* **113,** 5194–5261 (2013).
9. Yan, J., Bloom, M., Bae, S. C., Luijten, E. & Granick, S. Linking synchronization to self-assembly using magnetic Janus colloids. *Nature* **491,** 578–581 (2012).
10. Papadopoulos, P., Mammen, L., Deng, X., Vollmer, D. & Butt, H. J. How superhydrophobicity breaks down. *Proc. Natl Acad. Sci. USA* **110,** 3254–3258 (2013).
11. Verho, T. *et al.* Mechanically durable superhydrophobic surfaces. *Adv. Mater.* **23,** 673–678 (2011).
12. Wang, S. & Jiang, L. Definition of superhydrophobic states. *Adv. Mater.* **19,** 3423–3424 (2007).
13. Quéré, D. Wetting and roughness. *Annu. Rev. Mater. Res.* **38,** 71–99 (2008).
14. Whyman, G. & Bormashenko, E. How to make the Cassie wetting state stable? *Langmuir* **27,** 8171–8176 (2011).
15. Tyrrell, J. W. G. & Attard, P. Images of nanobubbles on hydrophobic surfaces and their interactions. *Phys. Rev. Lett.* **87,** 176104 (2001).
16. Mao, M., Zhang, J. H., Yoon, R. H. & Ducker, W. A. Is there a thin film of air at the interface between water and smooth hydrophobic solids? *Langmuir* **20,** 1843–1849 (2004).
17. Martines, E. *et al.* Air-trapping on biocompatible nanopatterns. *Langmuir* **22,** 11230–11233 (2006).
18. Poetes, R., Holtzmann, K., Franze, K. & Steiner, U. Metastable underwater superhydrophobicity. *Phys. Rev. Lett.* **105,** 166104 (2010).
19. Tang, Z. Y., Kotov, N. A. & Giersig, M. Spontaneous organization of single CdTe nanoparticles into luminescent nanowires. *Science* **297,** 237–240 (2002).
20. Tang, Z. Y., Zhang, Z. L., Wang, Y., Glotzer, S. C. & Kotov, N. A. Self-assembly of CdTe nanocrystals into free-floating sheets. *Science* **314,** 274–278 (2006).
21. Dong, A. G., Chen, J., Vora, P. M., Kikkawa, J. M. & Murray, C. B. Binary nanocrystal superlattice membranes self-assembled at the liquid–air interface. *Nature* **466,** 474–477 (2010).
22. Takahashi, M. Zeta potential of microbubbles in aqueous solutions: electrical properties of the gas-water interface. *J. Phys. Chem. B* **109,** 21858–21864 (2005).
23. Graciaa, A., Morel, G., Saulner, P., Lachaise, J. & Schechter, R. S. The zeta-potential of gas-bubbles. *J. Colloid Interface Sci.* **172,** 131–136 (1995).
24. Beattie, J. K., Djerdjev, A. N. & Warr, G. G. The surface of neat water is basic. *Faraday Discuss.* **141,** 31–39 (2009).
25. Beattie, J. K. & Djerdjev, A. M. The pristine oil/water interface: surfactant-free hydroxide-charged emulsions. *Angew. Chem. Int. Ed.* **43,** 3568–3571 (2004).
26. Huang, R. X., Carney, R. P., Stellacci, F. & Lau, B. L. T. Colloidal stability of self-assembled mono layer-coated gold nanoparticles: the effects of surface compositional and structural heterogeneity. *Langmuir* **29,** 11560–11566 (2013).
27. Saltzman, W. M. & Torchilin, V. *Drug Delivery Systems* (McGraw-Hill, 2008).
28. Zhou, H. *et al.* Self-assembly mechanism of spiky magnetoplasmonic supraparticles. *Adv. Funct. Mater.* **24,** 1439–1448 (2014).
29. Hollingsworth, A., Leunissen, M., Irvine, W., Chaikin, P. & van Blaaderen, A. Charged colloids in low polar solvents. *Bull. Am. Phys. Soc.* **53,** abstr. L9.00012 (2008).

Supplementary Information is available in the online version of the paper.

Acknowledgements This material is based on work partially supported by the Center for Solar and Thermal Energy Conversion, an Energy Frontier Research Center funded by the US Department of Energy, Office of Science, Office of Basic Energy Sciences under award number DE-SC0000957. We acknowledge support from the US NSF under grant ECS-0601345, CBET 0933384, CBET 0932823 and CBET 1036672. The work is also partly supported by the US Department of Defense under grant awards nos W911NF-10-1-0518, MURI W911NF-12-1-0407 and MURI W911NF-12-1-0407. We want express our appreciation to N. Walter for his leadership in organizing the SMART Center at the University of Michigan; J. Young Kim, Q. Che and X. Lu for help with the synthesis of CdTe nanoparticles; D. Bukharina for help with synthesis of hedgehog particles and SEM imaging of samples for dispersions in hydrophobic solvents; and D. Sorenson for assistance with TEM imaging of nanoparticle assemblies on OTMS-HPs. We also want to express our appreciation of H. Yu and G. Khan, who calculated van der Waals interactions of ZnO nanorods using the coupled dipole method. The guidance of C. Silvera Batista in this process is also much appreciated.

Author Contributions N.K. had the idea for the project. N.K. and J.H.B. designed the experiments. J.H.B. designed and made the hedgehog particles, did the experiments and did the calculations of the pairwise interaction potential between the hedgehog particles. J.H.B. and B.Y. did the initial design of the hedgehog particles. Y.W. did biological experiments and helped to make the hedgehog particles. S.O.T. made the Fourier transform infrared spectroscopy measurements and helped to make the hedgehog particles. J.D.H. did confocal microscopy using an Olympus IX81 inverted with an ISS Alba 5 to detect concentric mesoscale shells on hedgehog particles indicating differences in refractive indices.

Author Information Reprints and permissions information is available at www.nature.com/reprints. The authors declare no competing financial interests. Readers are welcome to comment on the online version of the paper. Correspondence and requests for materials should be addressed to N.K. (kotov@umich.edu).